Electronic structure of highly ordered Sr_2FeMoO_6: XPS and XES studies

2005 J. Phys.: Condens. Matter 17 4309

(http://iopscience.iop.org/0953-8984/17/27/007)

INSTITUTE OF PHYSICS PUBLISHING JOURNAL OF PHYSICS: CONDENSED MATTER

J. Phys.: Condens. Matter **17** (2005) 4309–4317 doi:10.1088/0953-8984/17/27/007

Electronic structure of highly ordered Sr_2FeMoO_6: XPS and XES studies

K Kuepper[1], M Kadiroğlu[1], A V Postnikov[2,3], K C Prince[4,5], M Matteucci[6], V R Galakhov[3], H Hesse[1], G Borstel[1] and M Neumann[1]

[1] Department of Physics, University of Osnabrück, D-49069 Osnabrück, Germany
[2] Institut für Festkörperforschung—Forschungszentrum Jülich, D-52425 Jülich, Germany
[3] Institute of Metal Physics, Russian Academy of Sciences—Ural Division, 620219 Yekaterinburg GSP-170, Russia
[4] Sincrotrone Trieste, km 163.5, in Area Science Park, I-34012 Basovizza (Trieste), Italy
[5] INFM–TASC, Laboratorio ELETTRA, I-34012 Basovizza (Trieste), Italy
[6] ICGEB—Area Science Park, Padriciano 99, 34012 Trieste, Italy

E-mail: kkuepper@uos.de

Received 2 February 2005, in final form 31 May 2005
Published 24 June 2005
Online at stacks.iop.org/JPhysCM/17/4309

Abstract

We have investigated the partial densities of states of Sr_2FeMoO_6 by applying soft x-ray emission spectroscopy (XES) to the Fe L, the Mo M and the O K edges. We discuss the results in the light of complementary measurements of the valence band by means of x-ray photoelectron spectroscopy (XPS) and first-principles generalized gradient approximation (GGA) and LDA + U band structure calculations.

1. Introduction

The manganites $La_{1-x}A_xMnO_3$ (A = Ca, Sr, Ba) have drawn much attention since the discovery of colossal magnetoresistance (CMR), which makes these materials interesting candidates for applications like, for example, the next generation of computer hard disk read heads [1–3]. More recently, huge magnetoresistance (MR) phenomena have also been reported for the double perovskite Sr_2FeMoO_6 [4]. More strictly speaking, Sr_2FeMoO_6 is a tunnelling magnetoresistance compound, with conductivity driven by the tunnelling of the charge carriers across insulating barriers [5, 6]. Due to its high Curie temperature of about 420 K and a substantial MR effect even at room temperature in a relatively low field, Sr_2FeMoO_6 is a promising model compound for applications in magneto-electronics and related industrial fields. In order to optimize the intricate magneto-resisting properties, these materials should be half-metallic, meaning the presence of a band gap in one spin direction and its absence in the other one [7]. For the investigation of these properties the techniques of x-ray and photoelectron spectroscopy are powerful tools, in particular in combination with first-principles electronic

structure calculations. Although various attempts to determine the electronic structure and to probe the correlation effects of Sr_2FeMoO_6 have been undertaken, the discussion of this point is still controversial [4, 8, 5, 9, 10]. Very different results have been reported, which in any case point out the importance of intra-atomic correlation at the Fe site. In simple terms, for example within the LDA + U approach [11], these effects are cast into a single parameter U, which has a meaning of the screened Coulomb interaction. With U one is bringing in some amount of Hubbard-model-like treatment on top of the conventional density functional theory (DFT) approach. In calculations done so far, it is argued for values of $U \simeq 4$ eV for the Fe 3d shell [9, 10], but also a U term for the O 2p orbitals has been introduced in a Hartree–Fock-type calculation by Ray *et al* [9]. In contrast, Saitoh *et al* have adopted significantly smaller values of U for the Fe 3d orbitals [5].

It should be noted that many previous calculations have been done with the linear muffin-tin orbital (LMTO) method, which is not very accurate in treating loosely, or inhomogeneously packed, systems, such as for example perovskite-type crystals. This is due to the use of the atomic-sphere approximation (ASA). The spherical averaging of potential within large, overlapping and space-filling atomic spheres is known to spoil the accuracy of the band structure. Another problem for the LMTO-ASA is the treatment of shallow semicore states (Sr 4p in the present case), which must be either attributed to the non-hybridizing core or treated as valence states. In the latter case the Sr 4p states have to be included into the basis at the expense of vacant Sr 5p states. Both possibilities are corrupting the accuracy of the DFT calculation. These technical limitations do not appear in full-potential schemes like the augmented plane wave method (APW), which was used in our present study. In this context it is noteworthy that a recent Compton profile study [6] was reported to be in good agreement with calculations by the full-potential linearized augmented plane-wave method without invoking any special treatment of the intra-atomic correlation beyond the conventional generalized gradient approximation (GGA).

The novelty of the present work is that it grasps the complete experimental picture of the total density of states (tDOS) and the partial densities of states (pDOS) of Sr_2FeMoO_6 obtained by means of x-ray photoelectron spectroscopy (XPS) and x-ray emission spectroscopy (XES). We compare these x-ray spectroscopic studies with *ab initio* band structure calculations. The latter have been performed within the DFT, using a full-potential augmented plane wave method. Moreover, as in some calculations cited above, but now on a computationally more accurate basis, we considered a treatment of the on-site Coulomb correlation beyond the 'conventional' scheme for the exchange–correlation, which was the GGA in our case, by making use of the LDA + U method. We tried different values of the phenomenological on-site Coulomb correlation parameter U for the Fe 3d shell and conclude that Sr_2FeMoO_6 is a moderately correlated compound; the best agreement between experiment and theory is found within the LDA + U scheme, adopting a U of 2.0 eV for the Fe 3d electrons. This is less than generally believed to be appropriate for more ionic iron oxides. No such correlation effects have been invoked for the Mo 4d electrons and the O 2p electrons.

2. Experimental and theoretical details

High-quality Sr_2FeMoO_6 polycrystals were produced by solid-state reaction. The powder was annealed at 1200 °C in a 99% Ar/1% H_2 atmosphere. X-ray analysis was used to check the structural quality and single-phase nature of the specimens, especially with respect to the antisite defect concentration. The best sample was found to have only ≈3% antisite concentration and a saturation magnetization of 3.5 μ_B [12]. All the following experiments were performed using this sample.

The XES spectra were measured at room temperature at the Advanced Light Source, beamline 8.0.1 using the x-ray fluorescence end station of the University of Tennessee at Knoxville [13]. Photons with an energy of 450–800 eV were provided to the end station via a spherical 925 lines mm^{-1} grating monochromator. The iron L, molybdenum M and oxygen K XES spectra were calibrated using a reference sample of pure Fe metal, Mo metal and MgO, respectively. The excitation energies were set to 800 eV for the Fe L edge, to 600 eV for the O K edge and to 500 eV for the Mo M edge for the measurements on the sample as well as for the corresponding calibration spectra. The overall resolution (beamline plus spectrometer) was set to around 1 eV for the O K and the Fe L edges. For the Mo M edge spectrum the beamline and spectrometer slits had to be opened due to the very low fluorescence intensity, resulting in a spectrometer resolution of about 2 eV. The sample was scraped in air with a diamond file in order to reduce surface contamination just before mounting in the transfer chamber. X-ray emission probes the sample to depths of tens or hundreds of nanometres and is bulk sensitive in the present study.

The XPS valence band was recorded using a PHI 5600CI multi-technique spectrometer with monochromatic Al Kα ($h\nu = 1486.6$ eV) radiation of 0.3 eV at full width of half maximum (FWHM), and with the sample at room temperature. The overall resolution of the spectrometer is 1.5% of the pass energy of the analyser, 0.35 eV in the present case. The spectrometer was calibrated using an Au foil as a reference sample (the binding energy of the Au $f_{7/2}$ core level is 84.0 eV [14]). To get a surface free of contamination, the sample was fractured *in situ*.

Regarding the calculations, we used the full-potential augmented plane wave method as implemented in the WIEN2k code [15]. The lattice parameters of the body-centred tetragonal unit cell used in the calculation were $a = 5.5706$ Å and $c = 7.8858$ Å (i.e. the base diagonal and the doubled length of the primative perovskite cell), according to [12]. Muffin-tin radii of 2.0 Bohr (Sr), 1.90 Bohr (Fe, Mo) and 1.6 Bohr (O) were used, with otherwise 'default' WIEN2k cut-offs for the basis function and charge density expansions ($RK_{max} = 7.0$, $G_{max} = 14.0$). We did not try to optimize lattice constants or internal coordinates; that would have required checking the convergency of results with respect to these cut-offs. For the exchange–correlation potential, we used the GGA-flavour known as 'Perdew-Wang 91', as discussed at length by Perdew *et al* [16]. Moreover, in order to describe the effects of intra-atomic correlation (presumably strong within the localized Fe 3d shell) beyond the conventional local density approximation (LDA) or GGA treatment, we allowed in some calculations the inclusion of an orbital-dependent potential of the type implementing the 'LDA + U' approach by Anisimov *et al* [11]; in particular (among many known variants thereof), the formalism outlined in [11, 17, 18]. The values of the Coulomb (U) and exchange (J) parameters entering this formalism were taken to be $J = 0.07$ Ryd, as routinely recommended for Fe in a number of similar calculations, and $U = 2$–4 eV (see the discussion below). The inclusion of spin–orbit interaction was tested and found not to affect the calculated DOS or energy bands in any noticeable way. The DOS discussed below has been calculated with $10 \times 10 \times 10$ divisions of the Brillouin zone.

3. Results and discussion

In figure 1 the XPS valence band of Sr_2FeMoO_6 is compared with results of different band structure calculations. The experimental valence band region comprises five distinct features labelled a–e. Features a and b are located around E_F, -1 eV on an energy loss scale, followed by a shoulder around -3 eV (c), a local maximum around -4 eV (d), and finally a rather broad absolute maximum in intensity (feature e) is located between -6.5 and -7.5 eV. We compare

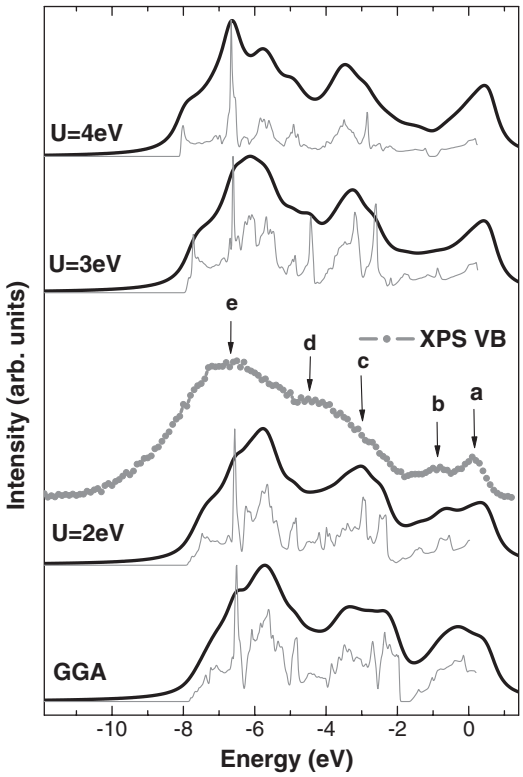

Figure 1. The XPS valence band of Sr_2FeMoO_6 (circles), compared with LDA+U calculations for different values of U (thin solid lines). The calculated total densities of states have been weighted with the corresponding photoionization cross-sections [19] and broadened with the spectrometer resolution (bold lines) for direct comparison with the experiment.

the experiment with the results of different *ab initio* band structure approaches, namely the total densities of states from a GGA calculation and also using different values for the on-site Coulomb potential U (see figure 1).

As the electronic structure of Sr_2FeMoO_6 has been calculated earlier, albeit with less accurate methods, we refer to its main features only briefly. Our main objective in the present work is to provide an adequate description of observed XPS and x-ray emission spectra, taking into account relevant weighting factors applied to the pDOS, and hence offer a plausible interpretation of them. The U parameter of the LDA + U approach is used as adjustable, in the search for the best possible agreement with experiment. We then discuss the calculated results corresponding to $U = 2$ eV, the value apparently yielding the best agreement with experiment, in more detail.

The valence band, which is probed by x-ray photoelectron spectroscopy, is mainly constituted by Fe 3d, Mo 4d and O 2p states. They have different photoionization cross-sections, which should be taken into account for weighting the corresponding atom-resolved contributions to the total DOS, as the simplest approximation of the measured spectra. Specifically, we took the relative photoionization cross-section values, corresponding to the excitation energy of 1486.6 eV, from [19]. The weights tabulated therein, which refer to each respective electronic shell as a whole, were normalized to a single electron and then multiplied with partial densities of states $g(E)$ and with the number of atoms of each type in the unit cell,

giving the calculated spectral intensity function $G_{\mathrm{tot}}(E)$:

$$G_{\mathrm{tot}} = 1 \cdot 0.017\,15 \cdot g_{\mathrm{Fe\ 3d}} + 1 \cdot 0.0315 \cdot g_{\mathrm{Mo\ 4d}} + 6 \cdot 0.003\,225 \cdot g_{\mathrm{O\ 2p}} + 2 \cdot 0.13 \cdot g_{\mathrm{Sr\ 4p}}.$$

The weighted valence band densities, for several trial U values, are those shown in figure 1 in comparison with the experimental spectrum.

All the calculated tDOS spectra reproduce the general structure of the measured XPS valence band correctly and better than previously published results [5, 10]—probably due to the superior accuracy of the present calculational method. Between the present calculations done with different U values, one notes differences in the positions of spectral features and in their relative intensity.

The a and b features are rather well reproduced already with the simple GGA ($U = 0$). However, the calculated intensity of band a is higher than that of band b, in contrast to the experimental result. At the opposite extreme, the LDA + U calculation with $U = 4$ eV predicts a much too narrow peak (of mostly Fe 3d character) just below the Fermi level, thus implying an 'unphysically' localized state. The calculation with the intermediate value of $U = 2$ eV reproduces the a and b features rather well, notably their relative intensities, and offers an acceptable description of features c to e. We note that the c feature seems to be overestimated in the simple GGA calculation, but that this is in part corrected in the LDA + U scheme.

There are still problems with the positions of the lower peaks: the theory predicts that the c, d, e features are 1–1.5 eV less bound, as compared to the experimental values. This trend is common in the density functional theory (DFT) when Kohn–Sham eigenvalues are compared with experimental excitation energies: an emitted electron leaves a hole behind, that enhances its binding energy, an effect which is stronger for more localized states and not accounted for in a conventional band structure calculation. The '+U' correction corrects for this effect, although for a different reason: each single correlated electron (which experiences the Coulomb correction to the potential) of the total N electrons feels the repulsion of other $N - 1$ electrons. In a conventional DFT treatment, in contrast, an electron feels the Coulomb repulsion from the charge density corresponding to all N electrons, with just an 'average' exchange–correlation hole dug in it. This would usually result in higher energy, due to a spurious self-interaction. The difference in energies between the two cases becomes larger for more localized states. Therefore the LDA + U approach might serve as a tool to model higher localization of relevant states and so to displace them close to energies consistent with spectroscopy. This would indeed happen for the lower peaks in the DOS of the current compound, assuming a U value of 4 eV (as shown in figure 1), or larger. Apparently the LDA + U treatment with a single, energy-independent U parameter is too simplistic to provide a good overall description of the XPS spectrum. However, we retain a moderate value $U = 2$ eV, which still offers a certain improvement over the conventional DFT description.

We do not wish to create the impression that we advocate the $U = 2$ eV value against the $U = 3$ eV. Rather, the finding is that the correlation effects remain moderate here, in contrast to other more ionic oxides. It is noteworthy that such a moderate value of U was favoured earlier for the LDA + U calculations on haematite Fe_2O_3 [20]. However, much larger values were under discussion for FeO, e.g., $U = 5.1$ eV by Mazin and Anisimov [21], or 4.6 eV by Pickett *et al* [22], and also $U = 4.51$ eV was found to be optimal for Fe_3O_4 by Anisimov *et al* [23].

An interesting property of Sr_2FeMoO_6, according to band structure calculations, is that it is a semi-metallic material. Its majority-spin band has an energy gap of about 1.2 eV around the Fermi level whereas the minority-spin band has small but finite density of states in this energy region; there is, however, a gap in the energy band spectrum of minority-spin states at $\approx$1.0 eV below the Fermi level. Such half-metallic behaviour is clearly present in a calculation

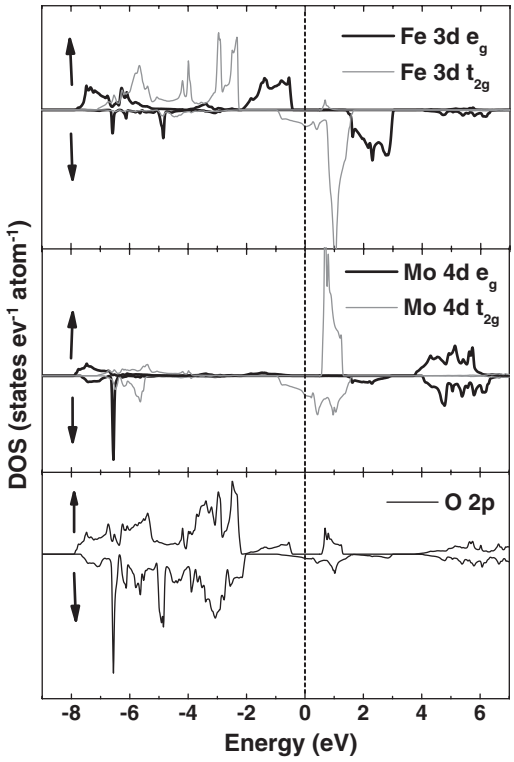

Figure 2. The spin-resolved, site-projected densities of states of the LDA + U ($U = 2$ eV) calculation for Sr_2FeMoO_6.

using the GGA for the exchange–correlation, resulting in a strictly integer magnetic moment ($4\ \mu_B$) per unit cell; the LDA calculation yields the half-metallicity only approximatively, as the Fermi level cuts the very top of the majority-spin band. The inclusion of the orbital-dependent potential within the LDA + U formalism opens the majority-spin band gap even further and thus 'stabilizes' the half-metallic state. Throughout the range of U values we tried, 0 to 4 eV, the band structure changes so that the centre of gravity of occupied states of the Fe 3d type is shifted downwards and that of vacant states upwards, as is common in LDA + U calculations. The majority-spin band gap opens slightly, and the magnetic moment per cell remains equal to $4\ \mu_B$, without pronounced quantitative changes.

Figure 2 shows the pDOS of Fe, Mo and Sr, calculated with $U = 2$ eV. These states hybridize to form a common valence band going down to ∼8 eV below the Fermi level. Sr is largely ionized, so its partial density of states higher in energy than the 4p semicore (at −17 eV, according to the calculation, and around −17.5 eV in the XPS spectrum) makes no noticeable contribution throughout the valence band. The O 2s states are even lower in energy and will also be excluded from the subsequent discussion.

The calculated pDOS helps us to understand the origin of different spectral features indicated in figure 1. The feature a in the XPS valence band can be attributed to overlapping Mo 4d and Fe 3d minority-spin states, which are mixed since they are degenerate in energy. The b peak comprises mainly the majority-spin Fe 3d (e_g) states, while feature c is mainly composed of the majority-spin Fe 3d (t_{2g}) states hybridized with the O 2p. The d feature can also be attributed to overlapping Fe 3d–O 2p states—however, with a strong minority-spin

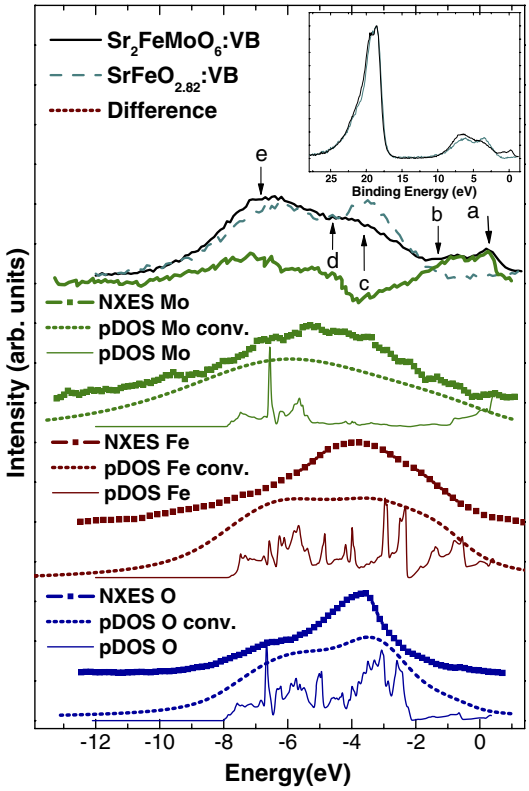

Figure 3. The XPS valence band and XES spectra of the Fe L edge, the Mo M and the O K edges of Sr_2FeMoO_6. The calculated densities of states are also shown (thin solid lines); the calculated pDOS have been also convoluted (thin dotted lines) with the overall experimental resolution (lifetime broadening plus spectrometer resolution). The XPS valence band of $SrFeO_{2.82}$ has been normalized to the Sr 4p XPS spectrum located around 17.5 eV of binding energy (see inset graph). The 'difference spectrum' of Sr_2FeMoO_6 and $SrFeO_{2.82}$ is also shown.

(This figure is in colour only in the electronic version)

contribution. Finally, the e feature contains both Fe 3d and Mo 4d contributions, the latter becoming gradually enhanced towards the conduction band bottom. A large photoionization cross section for the Mo 4d electrons accounts for the strength of the e peak in the resulting XPS valence band spectrum, despite their moderate participation in the total DOS.

Figure 3 displays the XPS valence band and the XES spectra of the Fe L, Mo M, and the O K edges. The XES spectra have been plotted on a common energy scale with the XPS valence band by using the corresponding XPS core level binding energies (710.6 eV for Fe $2p_{3/2}$, 529.4 eV for O 1s and 398.0 eV for Mo $3p_{3/2}$) for calibration. Hence, the XES spectra reflect the site-specific partial densities of states of the different elements in the compound which is symmetry-selected by the dipole selection rule, and broadened by the core–hole lifetime Γ_0 and the spectrometer resolution. Thus, in figure 3 there are also plotted the corresponding calculated partial densities of states (pDOS). In order to compare them directly with the experimental data they were broadened with the experimental resolution. The convolution was performed in two steps. In the first step a lifetime broadening of 0.5 eV was assumed for the O K and the Fe L edge emission spectra, and 2 eV for the Mo M edge emission spectrum. In the second step a further broadening accounting for the spectrometer

resolution was introduced, assuming a spectrometer resolution of 1 eV for the oxygen and the iron spectra, and 2 eV for that of molybdenum. According to the XES, the Fe 3d states are present from the Fermi level to around −8 eV binding energy; the maximum intensity is reached around −3.5 eV, corresponding to band c in the XPS valence band. The Fe L edge XES also indicates that the Fe 3d states extend over the whole valence band region; hence, the iron states are not extremely localized in energy. They exhibit a pronounced hybridization with O 2p states and, due to sharing a common oxygen neighbour with Mo atoms, show a number of features at the same energies (around E_F and also at −4 to −8 eV, bands c–e). The experimental XES results for iron and oxygen are also supported by the calculated (summed up over spin) densities of the Fe 3d and O 2p states, as seen from figure 3. For oxygen a very good agreement between experiment and theory is achieved. The deviations of the high-energy peak ($\sim$ −6.5 eV) of the Fe L edge XES and the convoluted calculation may be due to the presence of some correlation and multiplet effects in the experimental spectrum.

Finally, the Mo 4d XES spectrum spans the energy range from E_F to about −9 eV, with a rather broad maximum between −6 and −7 eV. In contrast the calculation suggests the presence of Mo 4d contributions around the Fermi level and in the region between −5 and −8 eV with a sharp maximum close to −7 eV. This difference is likely to be due to the rather high core–hole lifetime Γ_0 of metal 3p states, 2–4 eV estimated from the total atomic transition rates [24], and the broadened calculation, assuming such a lifetime broadening is in much better agreement with the experiment. In contrast one finds a value of around $\Gamma_0 = 0.4$ eV for the Fe $2p_{3/2}$ state [25].

We also compare the XPS valence band of Sr_2FeMoO_6 with that of $SrFeO_{2.82}$ as a reference. Since the amount of Sr is the same in both compounds we can normalize the XPS valence band spectra to the Sr 4p peak located around 17.5 eV binding energy scale (inset in figure 3). By subtraction of the $SrFeO_{2.82}$ valence band from that of Sr_2FeMoO_6, we obtain the curve labelled as 'Difference'. The residual then mainly reflects the Mo 4d contributions to the valence band of Sr_2FeMoO_6. According to theory features a and b are also formed by Fe 3d states and not only by Mo 4d states. The investigation of the Mo 4d states by means of this residual is limited by the fact that $SrFeO_{2.82}$ has a stoichiometry close to $SrFeO_3$, an antiferromagnetic insulator with Fe^{4+} ions compared to the half-metal Sr_2FeMoO_6, were the iron has a mixed Fe^{2+}/Fe^{3+} valency. The difference spectrum also contains a negative contribution between −2 and −3.5 eV which reflects parts of the Fe 3d density of states of $SrFeO_{2.82}$. The electronic structure of $SrFeO_{3-\delta}$ will be discussed in detail elsewhere [26]. Considering these facts the Mo 4d contribution to the valence band of Sr_2FeMoO_6, in particular the states around E_F and the low lying states between −6 and −8 eV, are nicely reproduced by the difference spectrum.

4. Conclusions

Our combined experimental and theoretical investigation of the total and partial densities of valence band states of Sr_2FeMoO_6 leads to the conclusion that Fe 3d–O 2p hybridization effects as well as Fe 3d and Mo 4d down-spin states near E_F play essential roles in determining the properties of this material. In addition, the Coulomb correlation (U) is particularly important for the Fe 3d electrons. We have presented a detailed x-ray spectroscopic study of the electronic structure of highly ordered Sr_2FeMoO_6 and compared these experimental results with different first-principles band structure calculations. The XPS valence band comprises five distinct features. The region near the Fermi level is dominated by energetically overlapping Mo 4d t_{2g} and Fe 3d t_{2g} spin-down states, which are also responsible for the half-metallic character of Sr_2FeMoO_6. Between −2 and −3.5 eV the valence band is dominated by Fe t_{2g} (spin-up) states. The lower-lying features can be attributed to strongly overlapping Fe 3d, O 2p and

Mo 4d states. In particular, the Fe 3d states are not extremely localized, and we find evidence that charge transfer between Fe 3d and O 2p states plays an essential role. In conclusion, Sr_2FeMoO_6 can be described as a moderately correlated compound. Assuming an effective potential $U_{dd} = 2.0$ eV for the Fe 3d electrons and invoking no on-site correlation energy for the Mo 4d and O 2p states leads to a satisfactory overall agreement between experiment and theory. However, the treatment of correlation effects within the Fe 3d shell within the LDA + U approach with just one single correlation parameter is too simplistic to recover a fully satisfactory description of all features of the observed spectra.

Acknowledgments

Financial support by the PhD program of Lower Saxony, Germany, is gratefully acknowledged. VRG and AVP acknowledge financial support of the Russian Foundation for Basic Research (Grant No 04-03-96092-Ural) and by the Research Council of the President of the Russian Federation (Grants NSH-1026.2003.2).

References

[1] von Helmolt R, Wecker J, Holzapfel B, Schultz L and Samwer K 1993 *Phys. Rev. Lett.* **71** 2331
[2] Millis A J 1998 *Nature* **392** 147
[3] Tokura Y and Nagaosa N 2000 *Science* **288** 462
[4] Kobayashi K L, Kimura T, Sawada H, Terakura K and Tokura Y 1998 *Nature* **395** 677
[5] Saitoh T, Nakatake N, Kakizaki A, Nakajima H, Moritomo O, Xu Sh, Moritomo Y, Hamada N and Aiura Y 2002 *Phys. Rev.* B **66** 035112
[6] Deb A, Hiraoka N, Ituo M, Sakurai Y, Koizumi A, Tomioka Y and Tokura Y 2004 *Phys. Rev.* B **70** 104411
[7] Park J H, Vescovo E, Kim H J, Kwon C, Ramesh R and Venkatesan T 1998 *Nature* **392** 794
[8] Solovyev I V 2002 *Phys. Rev.* B **65** 144446
[9] Ray S, Mahadevan P, Kumar A, Sarma D D, Cimino R, Pedio M, Ferrari L and Pesci A 2003 *Phys. Rev.* B **67** 085109
[10] Saha-Dasgupta T and Sarma D D 2001 *Phys. Rev.* B **64** 064408
[11] Anisimov V I, Aryasetiawan F and Lichtenstein A I 1997 *J. Phys.: Condens. Matter* **9** 767–808
[12] Kuepper K, Balasz I, Hesse H, Winiarski A, Prince K C, Matteucci M, Wett D, Szargan R, Burzo E and Neumann M 2004 *Phys. Status Solidi* a **201** 3252
[13] Jia J J, Callcott T A, Yurkas J, Ellis A W, Himpsel F J, Samant M G, Stöhr G, Ederer D L, Carlisle J A, Hudson E A, Terminello L J, Shuh D K and Perera R C C 1995 *Rev. Sci. Instrum.* **66** 1394
[14] Chastain J 1992 *Handbook of X-ray Photoelectron Spectroscopy* (Eden Prairie: Perkin Elmer Corporation)
[15] Blaha P, Schwarz K H, Madsen G K H, Kvasnicka D and Luitz J 2001 Improved and updated Unix version of the original copyrighted WIEN-code which was published by
Blaha P, Schwarz K, Sorantin P and Trickey S B 1990 *Comput. Phys. Commun.* **59** 339
[16] Perdew J P, Chevary J A, Vosko S H, Jackson K A, Pederson M R, Singh D J and Fiolhais C 1992 *Phys. Rev.* B **46** 6671
[17] Anisimov V I, Korotin M A, Zaanen J and Andersen O K 1992 *Phys. Rev. Lett.* **68** 345
[18] Liechtenstein A I, Anisimov V I and Zaanen J 1995 *Phys. Rev.* B **52** R5467–70
[19] Scofield J H 1976 *J. Electron Spectrosc. Relat. Phenom.* **8** 129
[20] Punkkinen M P J, Kokko K, Hergert W and Väyrynen I J 1999 *J. Phys.: Condens. Matter* **11** 2341
[21] Mazin I I and Anisimov V I 1997 *Phys. Rev.* B **55** 12822
[22] Pickett W E, Erwin S C and Ethridge E C 1998 *Phys. Rev.* B **58** 1201
[23] Anisimov V I, Elfimov I S, Hamada N and Terakura K 1996 *Phys. Rev.* B **54** 4387
[24] McGuire E J 1972 *Phys. Rev.* A **5** 1043
[25] McGuire E J 1971 *Phys. Rev.* A **3** 587
[26] Galakhov V R *et al* 2005 in preparation